JETIR.ORG ISSN: 2349-5162 | ESTD Year : 2014 | Monthly Issue

JOURNAL OF EMERGING TECHNOLOGIES AND INNOVATIVE RESEARCH (JETIR)

An International Scholarly Open Access, Peer-reviewed, Refereed Journal

Interconnection of AC-DC microgrids in grid-connected hybrid microgrid using UIPC in Neural Networks

K.Umamaheswara Reddy [1] Mr.Ramu[2] Mr.Ramesh[3]

[1](M.Tech Student, Department of Electrical and Electronics Engineering, Quba College of Engineering And Technology, Venkatachalam, Nellore. A.P, India)

[2](Head Of The Department, Department of Electrical and Electronics Engineering, Quba College of Engineering and Technology, Venkatachalam, Nellore. A.P, INDIA)

[3](Assistant Professor, Department of Electrical and Electronics Engineering, Quba College of Engineering and Technology, Venkatachalam, Nellore. A.P, INDIA)

Abstract:

This paper presents another methodology for power stream control of interconnected AC-DC microgrids in framework associated mixture microgrids dependent on actualizing an altered brought together interphase power regulator (UIPC). A normal matrix associated half breed microgrid including one AC microgrid and one DC microgrid is considered as examined framework. Rather than utilizing the equal associated power converters, these microgrids are interconnected utilizing an adjusted UIPC. As the principal commitment of this paper, the traditional structure of UIPC, which utilizes three force converters in each stage, is altered with the goal that a diminished number of intensity converters is executed for power trade control between AC-DC microgrids. The adjusted structure remembers one force converter for each stage, named as line power converter (LPC), and a force converter which manages the DC transport voltage, named as transport power converter (BPC) here. The AC microgrid is associated with the primary network through the LPCs which their DC transports are connected and can work in capacitance mode (CM) or inductance mode (IM). A fluffy rationale regulator is utilized in the control structure of the LPCs. The fluffy derivation framework is advanced dependent on H∞ sifting technique to lessen the blunders in enrollment capacities structure. Through the BPC, the DC voltage of LPCs is provided by the DC microgrid. In any case, since the DC microgrid voltage is given here by a PV framework, the DC interface voltage of the LPCs is fluctuating. Along these lines, as the subsequent commitment, to settle the DC connect variances, another nonlinear unsettling influence onlooker based hearty various surface sliding mode control (NDO-MS-SMC) procedure is introduced for DC side control of the BPC. The system response is also tested with Neural Network controller in place of existing fuzzy controller. The recreation results affirm the adequacy of the proposed power stream control technique of the improved UIPC for mixture microgrids.

I. INTRODUCTION

Over the previous ten years, the DC power assets, for example, photovoltaic (PV) frameworks, energy units (FCs), vitality stockpiling frameworks (ESSs) just as recently presented DC loads, for example, programmable DC electronic burdens and so forth., have entered into the customary force frameworks through DC microgrids [1]. Then again, the AC power assets, for example, wind turbines and so on just as the AC loads, for example, electrical engines, and so on. might be associated with the force frameworks through the AC microgrids [2-3]. Later on keen networks, the AC and DC microgrids including AC and DC power assets and burdens are coordinated as a cross breed framework called the half breed microgrids [4]. As a matter of fact, the AC and DC microgrids are interconnected through the force converters. This association permits the microgrids to trade power when required. The force converters are normally associated in corresponding to trade bigger measure of intensity and increment unwavering quality [5]. Fig. 1 shows the structure of a run of the mill matrix associated half breed microgrid. In this figure, the DC microgrid may incorporate PV frameworks, ESSs and related burdens, which are associated with a typical DC transport [6]. The AC microgrid may contain wind turbine, diesel generator and the AC loads which are associated with a typical AC transport [7]. The entire half and half microgrid might be associated with the force framework or separated [8]. As appeared in Fig. 1, the basic transports (joins) of two microgrids are interconnected through equal associated bidirectional force converters, called interlink power converters (ILCs) [9]. Be that as it may, there are some specialized difficulties in resembling power converters in crossover microgrids as follows [8-17]:

- The microgrids have diverse unique qualities, for example, extraordinary voltage levels, stage, recurrence, and force change.
- A mixture microgrid may incorporate a few microgrids. For instance, two AC microgrids and one DC microgrid. In such an arrangement with various elements, utilizing equal associated ILCs to trade power between microgrids is troublesome and confused since the voltage greatness and period of the basic transports of the microgrids must be the equivalent so as to abstain from flowing current between equal associated ILCs.

- The moved force among microgrids must be consistently partitioned among equal associated ILCs with equivalent force appraisals.
- The force sharing execution of the equal associated ILCs is influenced by change in the framework boundaries, for example, line impedance, load variety, and so on.
- If there is a flaw in a microgrid, the deficiency current might be shared non-consistently among ILCs since the shortcoming is a nonlinear wonder. In this circumstance, the current moving through the force converters is relied upon to cross the ostensible current constraints of the force converter and hence, it might be disconnected bringing about a significant decrease in traded power. This thus may bring about burden concealing in a microgrid or even precariousness.
- The intermittent behavior of some distributed generation (DG) units in microgrids causes many uncertainties in generated power and also oscillations in exchanged power among microgrids.
- The distortions in the AC microgrids, such as harmonics, result in phase difference between ILCs which in turn causes voltage drop [15].
- The parallel-connected ILCs may operate in different power factors. This causes voltage and power oscillations and affects the power sharing performance.

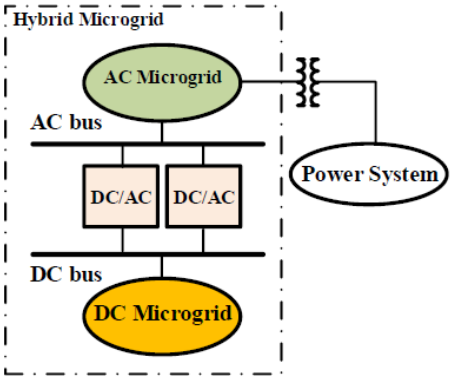

Fig. 1. A typical grid-connected hybrid microgrid

To tackle previously mentioned issues, numerous procedures and control techniques have been proposed in writing. In [12], a various leveled control system for equal associated bidirectional ILCs has been proposed. The foundation of the control strategy has been structured in fixed reference outline (SRF), without shared term among tomahawks, went with with consonant review. The value of this technique is that it is simple to actualize since it has been structured in the SRF. In [13], a hang control-based various leveled control technique has been proposed in which the principal control level has utilized a hang plot. In the DC side, the corresponding essential (PI) regulators have been actualized though the proportionalresonant (PR) regulator has been utilized at the AC side. The second control level has altered the wave, which had been created because of the primary level control activity, and the third control level has been utilized to associate the crossover microgrid with the utility. In [14], a shortcoming secured dynamic force control conspire has been proposed for network associated crossover microgrids. The technique has utilized a tunable scalar to differ the greatness of dynamic and receptive force motions. The creators in [15] have shown that the voltage unbalance brings about force vacillations. A control technique for parallelconnected ILCs has been proposed which has controlled the current of each force converter with the goal that the summation of all ILCs flows was adjusted. To this end, one of the ILCs has been considered as "excess" with higher evaluations. This makes the control plot expensive.

Likewise, the proposed technique is powerless against consonant bending and also, the plan is incapable to decrease the responsive force motions. In [16], a vigorous control plot has been intended for power sharing control between two equal associated inverters. The technique has utilized μ union examination to structure the current regulator of inverters. In [17], an ideal fragmentary request regulator has been intended for power sharing among two parallelconnected inverters. The scientists in [18] have given design, in view of the IEEE 1547.4-2011, for cross breed microgrids. A decentralized and self-advanced control framework for confined microgrids has been depicted in [19]. The control strategy has given neighborhood control activities with no correspondence joins which has made the strategy more solid. The Flexible AC transmission System (FACTS) gadgets have additionally been utilized to control power stream in AC transmission frameworks. In the current paper, utilizing UIPC is acquainted with control the traded power between microgrids just as fundamental framework in a cross breed microgrid. The Realities gadgets have been utilized in many force control applications with various control structures. In [20], the bound together force stream regulator (UPFC) has been utilized to upgrade voltage steadiness. Additionally, the ideal portion of UPFCs has been resolved utilizing hereditary calculation. The between line power stream regulator (IPFC) has been utilized in [21] to ideally control the moved force in a transmission line. The creators in [22] have executed the static VAr compensators (SVCs) to improve the force framework security with monetary investigation. The static simultaneous arrangement compensator (SSSC) has been applied in a transmission line which associates two territories in a force framework [23]. The SSSC has been compelling in traded power control between two territories. The UIPC has first been presented in [24]. It is an upgraded rendition of customary IPC (interphase power regulator) which utilizes the force converters rather than stage moving transformers in each stage. The adequacy of the UIPC in power stream control has been confirmed in [24].

This paper focuses on little scaled altered UIPC to control the traded power among microgrids just as primary network in a mixture microgrid condition. The primary commitments of this work include:

Rather than utilizing equal associated power converters which have many control issues [8-17], the UIPC is proposed to control the traded power among microgrids as well as fundamental network in a half and half microgrid. The regular structure of UIPC, which utilizes three force converters in each stage, is changed with the goal that a diminished number of intensity converters is executed for power trade control between AC-DC microgrids.

- Since the microgrids elements in a cross breed microgrid are not quite the same as the ordinary force framework elements, the issue of controlling the UIPC, with a DC microgrid associated its DC transport, would be a troublesome undertaking which is tended to by this work and another NDO-MS-SMC-based control technique is introduced for the DC side control of the BPC.

Accordingly, this examination accentuates on utilizing the UIPC as an elective answer for power stream control among numerous microgrids in half and half microgrids.

In contrast with the traditional equal associated power converters, the UIPC have the accompanying favorable circumstances:

- Control of traded power between microgrids without setting up lumbering limitations, for example, equivalent voltage extents, stages and so on., which are generally needed to interface the ILCs in equal.
- The UIPC, as appeared in [24], can undoubtedly restrict the flaw current without need to utilize an excess force converter as portrayed in [15]. This element makes the interconnection more dependable, cheap reasonably, and less convoluted in contrast with the control techniques, for example, the quick force control plot which has customarily been utilized for equal associated ILCs.
- Despite of equal associated ILCs which give direct electrical associations between microgrids, the proposed changed UIPC gives a voltage confinement include as shown in [24].
- The UIPC can control the DC transport voltage of the DC microgrid just as the AC transport voltage of the AC microgrid. This trademark was not given by utilizing the ordinary equal associated ILCs.

Along these lines, realizing all previously mentioned highlights, in this work a changed form of the UIPC is utilized to interconnect half and half microgrids. The remainder of this work is set up as follows: Section II portrays the adjusted UIPC. Segment III presents another aggravation eyewitness based powerful different surface sliding mode control procedure to determine the vacillations of the normal DC transport voltage of the altered UIPC. The reproduction results and correlation contextual analyses are depicted in Section IV. Finally, Section V accompanies finish of the work.

II. PROPOSED UIPC BASED STRUCTURE OF HYBRID MICROGRID AND DYNAMIC MODELING

This section describes the proposed hybrid microgrid topology focused on the UIPC. The dynamic model of the modified UIPC is also presented in this section. Fig. 2 illustrates the studied hybrid microgrid. As indicated, the grid-connected hybrid microgrid contains one AC microgrid and one DC microgrid which are interconnected through the UIPC. The AC microgrid, includes a diesel generator and related AC and DC loads. A PV system, a battery, and AC and DC loads exist in the DC microgrid. The loads, the PV system, and the battery are connected to the common DC bus (DC link).

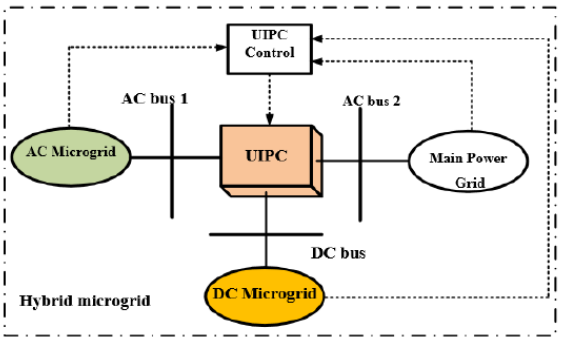

Fig. 2. Interconnection of AC-DC microgrids in grid-connected hybrid microgrid using UIPC

A. Conventional UIPC

The per-phase model of the UIPC has been described in [24] and indicated in Fig. 3. In this structure, the phase- moving transformers of the interphase power regulator (IPC) had been subbed by voltage source converters (VSCs). Along these lines, two AC transports, for example ..1 and ..2, are associated through three VSCs, for example VSC1, VSC2, and VSC3, in each stage. VSC1 and VSC2 go about as stage moving converters while VSC3 goes about as voltage controlling converter. VSC1 works in inductive mode and infuses the arrangement voltage ..... to the line through transformer T1. Then again, VSC2 works in capacitive mode and infuses the arrangement voltage ..... to the line through transformer T2. The third VSC, for example VSC3 is associated with one of the AC transports, here ..1, through transformer T3 and controls the AC voltage. The DC transport of all the VSCs is associated in equal and provided by a consistent capacitor. In this manner, the DC connect voltage ..... is liable for giving dynamic forces of each VSC. Accordingly, through stage edge control of VSC1 and VSC2, the traded power between the two AC transports would be controlled. More subtleties can be found in [24].

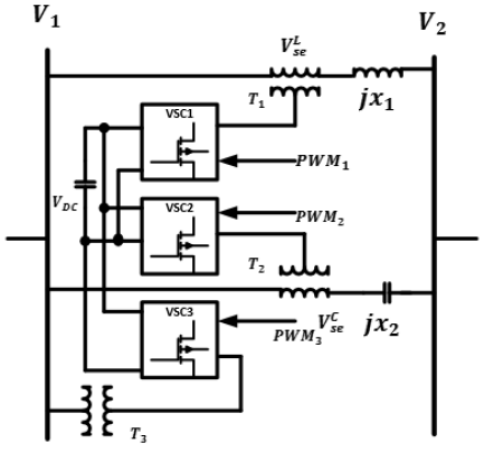

Fig. 3. Conventional structure of UIPC; each phase implements three power converters [24]

B. Proposed structure of UIPC

Firstly, the topology of the conventional UIPC, described in the previous subsection, will be modified. Then, the control strategy of the modified UIPC will be shown in the subsequent subsection. The conventional structure of UIPC, illustrated in Fig. 3, has the following deficiencies:

- Each phase implements three VSCs; therefore, to connect three phases of AC buses, one needs nine VCSs, and also nine power transformers which make the topology extensively costly.
- The DC links of all the VSCs in each phase are connected in parallel. However, as described in [12, 25], the VSCs with common DC links are inclined to make the common DC link voltage oscillatory when the output powers of VSCs change or when there is a disturbance on the system model, for example, change in a system parameter. The DC link voltage fluctuation is a major concern in VSCs with a common DC link. This issue has not been considered in [24].

To remove the abovementioned barriers, the modified UIPC model is proposed as indicated in Fig. 4. As shown, each phase just uses one power converter, named as $LPCj$, where $j\in\{1,2,3\}$ is the line number. These power converters, through transformers Tj, inject the series voltage $Vse\angle\varphi se=Vser+jVsei$ to each line, where $Vser$ and $Vsei$ are the real and imaginary parts of injected series voltage, respectively. The line impedance is $ZLj=RLj+jXLj$. Generally speaking, the injected series voltage is actually a controlled voltage source with the following general form:

$$V_{se} = K_A V_{DC} \angle K_P \varphi_{se}$$

where, KA and KP are voltage amplitude and phase coefficients, respectively. The voltage amplitude coefficient KA is indeed a function of pulse width modulation (PWM) strategy and the phase coefficient KP is ±1 and φse is usually equal to $\pi 2$. The switches $S1$and $S2$are anti-parallel thyristors and would be coordinated by the injected voltage phase angle through the control system. At each instant, only one of these switches conducts at each phase, depending on the phase angle sign. Whenever the voltage phase coefficient KP is equal to +1, the UIPC is in the inductive mode (IM) and $S1$ is on whereas $S2$ is off. In a similar way, when the phase coefficient KP is equal to -1, the UIPC is in the capacitive mode (CM) and $S1$ is off whereas $S2$ is on. Thus, the exchanged power between the two AC buses, i.e. $V1$ and $V2$, can be controlled. In Fig. 4, also notice that there is only one BPC for all phases. The DC bus of this BPC is then connected to the DC microgrid. The BPC, through transformer $TBPC$, is also connected to one of the AC buses (weaker AC bus, i.e. AC microgrid bus), here $V1$, to regulate the AC voltage and provide power exchange with the DC microgrid. The vector diagram of the system voltages considering the injected voltage of the proposed UIPC is shown in Fig. 5. According to this diagram one may obtain;

$$\varphi_{se}^{L} = \varphi_1 + \alpha_1$$
$$\varphi_{se}^{C} = \varphi_2 + \alpha_2$$

These angles are calculated by considering different operation modes of the UIPC, i.e. IM or CM. In Equations (2)-(3), $\varphi seL$and $\varphi seC$are the phase angle of the voltage at the middle point of the transmission line, when the UIPC operates in IM and CM modes, respectively.

According to complex power flow concept [26], the exchanged power between the two AC buses would be determined as follows:

$$S = V_2\left(\frac{V_1-V_2}{Z_L}\right)^* = \quad (4)$$
$$(V_2\cos\delta_2 + jV_2\sin\delta_2)\frac{(V_1\cos\delta_1+jV_1\sin\delta_1-V_2\cos\delta_2-jV_2\sin\delta_2)^*}{R_{L1}-jX_{L1}}$$

where, $\delta 1$and $\delta 2$ are the phase angles of the voltages $V1$ and $V2$, respectively. After some mathematical manipulations, Equation (4) can be written as follows:

$$P = \frac{R_{L1}V_1V_2(\cos\delta_1\cos\delta_2+\sin\delta_1\sin\delta_2+R_{L1}V_2^2)-X_{L1}V_1V_2(\cos\delta_1\sin\delta_2-\sin\delta_1\cos\delta_2)}{R_{L1}^2+X_{L1}^2} \quad (5)$$

$$Q = \frac{R_{L1}V_1V_2(\cos\delta_1\sin\delta_2-\sin\delta_1\cos\delta_2)+X_{L1}V_1V_2(\cos\delta_1\cos\delta_2+\sin\delta_1\sin\delta_2+X_{L1}V_2^2)}{R_{L1}^2+X_{L1}^2} \quad (6)$$

In microgrids, $RL1 \gg XL1$ and we get:

$$P = \frac{V_1V_2(\cos\delta_1\cos\delta_2+\sin\delta_1\sin\delta_2+R_{L1}V_2^2)}{R_{L1}} = \frac{V_1V_2}{R_{L1}}(\cos(\delta_1-\delta_2)+R_{L1}V_2^2) \quad (7)$$

$$Q = \frac{V_1V_2(\cos\delta_1\sin\delta_2-\sin\delta_1\cos\delta_2)}{R_{L1}} = \frac{V_1V_2}{R_{L1}}\sin(\delta_2-\delta_1) \quad (8)$$

Thus, the transferred active power is controlled by the voltage magnitudes of the AC buses whereas the reactive power is controlled by the phase angle difference. The voltage magnitude and phase angle difference are controlled by the proposed UIPC implying that the exchanged active and reactive powers between two AC buses would be controlled easily. Considering Fig. 6, to evaluate the effects of the injected voltage of the UIPC, and using Kirchhoff Voltage Law, we obtain:

$$V_1\angle\delta_1 - V_2\angle\delta_2 = (R_{L1}+jX_{L1})I + V_{se}\angle\varphi_{se} \quad (9)$$
$$= (R_{L1}+jX_{L1})\frac{P-jQ}{V_2^r-jV_2^i} + \left(V_{se}^r + jV_{se}^i\right) =$$
$$\left(\frac{V_2^r(R_{L1}P+X_{L1}Q)+(X_{L1}P-R_{L1}Q)}{(V_2^r)^2+(V_2^i)^2} + V_{se}^r\right)$$
$$+j\left(\frac{V_2^r(X_{L1}P-R_{L1}Q)+(R_{L1}P+X_{L1}Q)}{(V_2^r)^2+(V_2^i)^2} + V_{se}^i\right)$$

In the microgrids, $XL1P \cong RL1Q$ and we get:

$$V_1\angle\delta_1 - V_2\angle\delta_2 = \left(\frac{V_2^r(R_{L1}P+X_{L1}Q)}{(V_2^r)^2+(V_2^i)^2} + V_{se}^r\right) + jV_{se}^i \quad (10)$$

Also, $RL1P \gg XL1Q$ and we have:

$$V_1\angle\delta_1 - V_2\angle\delta_2 = \left(\frac{V_2^r+V_{se}^r\left((V_2^r)^2+(V_2^i)^2\right)}{(V_2^r)^2+(V_2^i)^2}\right) + jV_{se}^i \quad (11)$$

The exchanged power between the DC link and the AC link (..1) can be obtained using the power balance equation as follows:

$V_{DC}I_{DC}^{UIPC} = \frac{3}{2}V_1^d i_1^d$

where $IDCUIPC$is the current flowing in the DC link of the UIPC, and $V1d$ and $i1d$ are the d-axes voltage and current of the AC link, respectively.

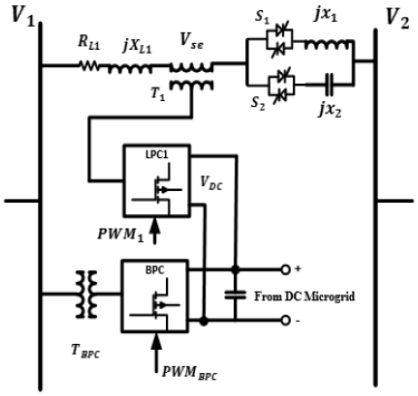

Fig. 4. Proposed topology of UIPC (each phase implements only one power converter, named as LPC)

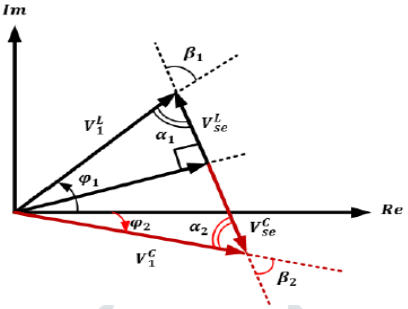

Fig. 5. Voltages when the proposed UIPC is involved

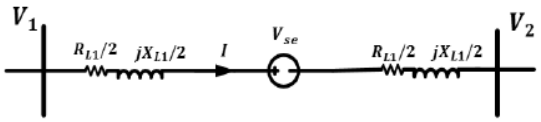

Fig. 6. Model of each phase of system considering injected voltage of proposed UIPC

The per-stage geography of the proposed UIPC based interconnected microgrids in the cross breed microgrid is delineated in Fig. 7. The general control structure of the proposed UIPC is additionally appeared in this figure. The control framework incorporates two subsystems: Series VSC control and NDO-MS-SMC based DC connect control. The Series VSC Control subsystem controls the infused voltage and switches $S1$and $S2$ and an ideal H∞ based fluffy rationale regulator is utilized its structure. This control subsystem is portrayed in the resulting subsection. The SMC based DC connect Control subsystem is liable for balancing out the normal DC interface voltage vacillations and depends on another aggravation spectator based hearty various surface sliding mode control system. This control structure technique is portrayed in the following area.

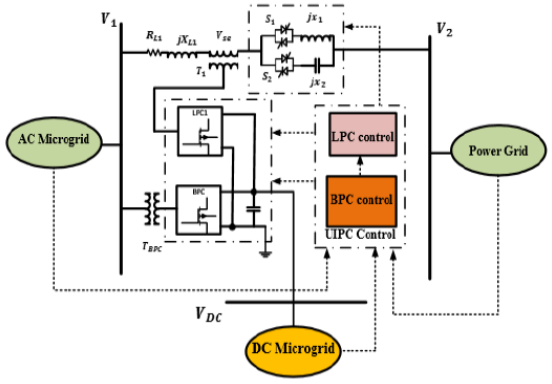

Fig. 7. Per-phase model of interconnection of AC-DC microgrids using the UIPC and control system of UIPC

Quickly, in contrast with the regular structure, the proposed UIPC geography has the accompanying benefits;

- Each stage just needs one LPC.
- Only one BPC is required in the three-stage structure. Subsequently, the general model needs four VSCs and three force transformers.
- The DC interface voltage is provided through the DC microgrid. This component empowers the UIPC to interconnect the AC and DC microgrids.
- An ideal fluffy rationale regulator is utilized in the control structure of the LPCs which lessens the mistakes.

C. Proposed control strategy for LPCs

As indicated by Fig. 7, the proposed control conspire for the proposed UIPC structure incorporates two control subsystems; LPCs control methodology and SMC based control plot for BPC. These control subsystems have control cooperations too. Fig. 8 shows the proposed control technique for each LPC at each stage. As appeared, the infused arrangement voltage and the line current are

estimated and scaled. At that point, to get the crucial parts of these scaled signs, a bandpass channel is utilized. The boundaries (move work) of this channel are resolved utilizing MATLAB [27], as follows:

- The voltage vacillations of the DC interface are damped utilizing an unsettling influence eyewitness based powerful different surface sliding mode control technique which is portrayed in the following segment.

$$T_f = \frac{190.10s}{s^2+190.10s+145321}$$

The root mean square (rms) values of the filtered signals are then obtained. The injected voltage error is given to the proposed optimal fuzzy logic controller (FLC). The phase of the injected voltage is measured using a PLL. Then, the sign of this phase, which is actually KP in Equation (1), is determined and based on this sign, it is concluded that the UIPC operates whether in IM mode or CM mode. Thus, the appropriate phase shift is applied; $+\pi 2$ for IM mode and $-\pi 2$ for CM mode. Furthermore, the switches $S1$ and $S2$are enabled/disabled based on the operation modes. The optimal FLC is designed based on H∞ filtering design procedure which has fully been described and validated in [28] by the authors of this work. As illustrated in Fig. 8, a DC link voltage signal is fed to the all LPCs control system for coordination. The error signal is then given to an optimal FLC. Therefore, the control signal (reference) for implementation in PWM unit is generated using these signals. Based on the PWM scheme, the amplitude of the injected voltage (through KA) is controlled, as given in Equation (1).

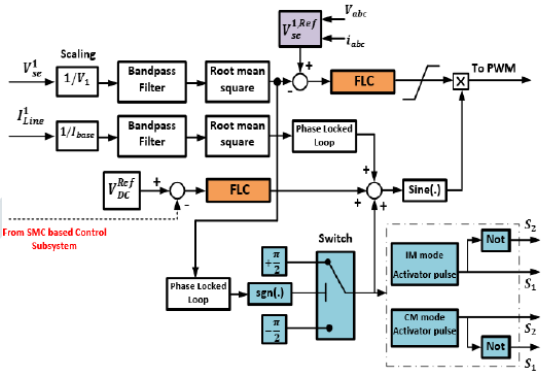

Fig. 8. Proposed control strategy for LPCs

III. PROPOSED NDO MULTIPLE SURFACE SMC BASED DC LINK VOLTAGE CONTROL OF UIPC

The DC links of the LPC and BPC are in parallel and connected to the common DC bus of the DC microgrid. As mentioned before, the DC link voltage would be unstable due to the output active power change of power converters, loads or PV system in the DC microgrid. Thus, a new NDO-MS-SMC is used in this section to control the DC link voltage of the proposed UIPC.

A. Structure of proposed control scheme

Fig. 9 shows the proposed control scheme for BPC. In fact, and as described earlier, the BPC is responsible to regulate the DC link and therefore, the proposed NDO-MS-SMC strategy is applied to the BPC. As shown in Fig. 9, the proposed control scheme includes three parts: 1- the voltage control loop 2- the current control loop and 3- the NDO. The NDO is responsible for estimating the uncertainties and power changes in the DC microgrid. Furthermore, the NDO caters a reference signal for the dead-time compensation unit and the current control loop. The voltage control loop uses optimal proportional-integral (PI) controllers accompanied by the feedforward power disturbance to catch up the constitutional delay nested in the dynamics of the current control loop and the proposed disturbance observer. The PI controllers in both current and voltage control loops are optimally tuned using the genetic algorithm (GA).

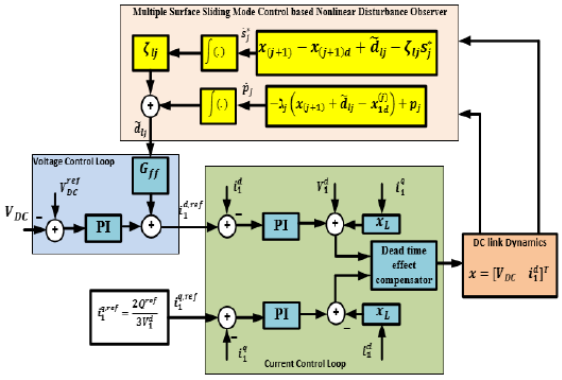

Fig. 9. Control of DC link of BPC based on new NDO-MS-SMC strategy

B. Dynamic model of nominal system

Firstly, the dynamic equations of the common DC link of BPC will be extracted without using any parametric uncertainty; so called the nominal model. Using Kirchhoff Current Law we get:

$$C\frac{dV_{DC}}{dt} = -I_{DC}^{UIPC} + I_{dist} \qquad (14)$$

where, C is the capacitor of the common DC link, and $Idist=IDCPV+IESS+IL$ is the disturbance current in which $IDCPV$ is the output DC current of the PV system, $IESS$ is the energy storage system (ESS) current (for example, a battery), and IL is the lumped DC loads current.

The BPC model in dq-frame can be expressed as follows [29]:

$$\begin{cases} V_o^d = V_1^d + L\left(\frac{di_1^{dt}}{dt}\right) + \omega L i_1^q + i_1^d R \\ V_0^q = L\left(\frac{di_1^q}{dt}\right) - \omega L i_1^d + i_1^q R \end{cases} \qquad (15)$$

Where, $Vo$and $V1$ are the output AC voltage of the BPC and AC bus to which the BPC is connected, respectively, ω is the angular frequency in rad/s, and L and R are the inductance and resistance of the output filter of the BPC, respectively.
Therefore, using Equations (12), (14), and (15) we obtain:

$$\begin{cases} \frac{dV_{DC}}{dt} = -\frac{3V_1^d i_1^d}{2CV_{DC}} + \frac{1}{C} I_{dist} \\ \frac{di_1^d}{dt} = \frac{V_o^d - V_1^d}{L} - \omega i_1^q - \frac{R}{L} i_1^d \end{cases}$$

Equation (17) indicates a system with nonlinear terms. This is the nominal model of the system.

C. Dynamic model of perturbed system

The uncertainties are considered on the capacitance of the DC link *C*, the disturbance current , and the inductance *L* as follows:

$$\frac{1}{C} = \frac{1}{\bar{C}(1+\rho_C\theta_C)} = \frac{1}{\bar{C}} - \frac{\rho_C}{\bar{C}}\theta_C(1+\rho_C\theta_C)^{-1} \quad (18)$$

$$\frac{1}{L} = \frac{1}{\bar{L}(1+\rho_L\theta_L)} = \frac{1}{\bar{L}} - \frac{\rho_L}{\bar{L}}\theta_L(1+\rho_L\theta_L)^{-1} \quad (19)$$

$$I_{dist} = \bar{I}_{dist}\left(1+\rho_{I_{dist}}\theta_{I_{dist}}\right) \quad (20)$$

where, $\bar{C}$, $\bar{L}$, and $\bar{I}dist$ are the nominal values of C, L, and $Idist$, respectively, and ρC, ρL, and $\rho Idist$ and θC, θL, and $\theta Idist$represent the probable perturbations on these parameters which are random numbers in the range of -1 to +1.
Introducing these perturbed parameters into the nominal system (17) we get:

$$\begin{aligned} \dot{x_1} &= \left(\frac{1}{\bar{C}} - \frac{\rho_C}{\bar{C}}\theta_C(1+\rho_C\theta_C)^{-1}\right)\left(-\frac{3V_1^d x_2}{2x_1}\right) \\ &+ \left(\frac{1}{\bar{C}} - \frac{\rho_C}{\bar{C}}\theta_C(1+\rho_C\theta_C)^{-1}\right)\left(\bar{I}_{dist}(1+\rho_{I_{dist}}\theta_{I_{dist}})\right) \quad (21) \\ &= -\frac{3V_1^d x_2}{2\bar{C}x_1} + \frac{\bar{I}_{dist}}{\bar{C}} + \left(\frac{3V_1^d x_2}{2x_1}\right)\rho_C\theta_C(1+\rho_C\theta_C)^{-1} + \\ &\frac{\bar{I}_{dist}}{\bar{C}}\rho_{I_{dist}}\theta_{I_{dist}} - \frac{\bar{I}_{dist}}{\bar{C}}\rho_C\theta_C(1+\rho_C\theta_C)^{-1}(1+\rho_{I_{dist}}\theta_{I_{dist}}) \end{aligned}$$

$$\begin{aligned} \dot{x_2} &= \left(\frac{1}{\bar{L}} - \frac{\rho_L}{\bar{L}}\theta_L(1+\rho_L L)^{-1}\right)\left(-Rx_2 + u - V_1^d\right) - \omega i_1^q \quad (22) \\ &= \frac{R}{\bar{L}}x_2 + \frac{u}{\bar{L}} - \frac{V_1^d}{\bar{L}} - \omega i_1^q + \frac{\rho_L\theta_L}{\bar{L}}(Rx_2 - u + V_1^d)(1+\rho_L\theta_L)^{-1} \end{aligned}$$

D. Design of NDO-MS-SMC

In this subsection, the proposed NDO-MS-SMC, indicated in Fig. 9, is designed by pursuing the following steps:
Step 1. Determine the perturbed system model as the standard form: To do this, Equations (21) and (22) should be rewritten using the following disturbance parameters:

$$d_1(x,t) = \frac{\bar{I}_{dist}}{\bar{C}} + \left(\frac{3V_1^d x_2}{2x_1}\right)\rho_C\theta_C(1+\rho_C\theta_C)^{-1} + \frac{\bar{I}_{dist}}{\bar{C}}\rho_{I_{dist}}\theta_{I_{dist}} - \frac{\bar{I}_{dist}}{\bar{C}}\rho_C\theta_C(1+\rho_C\theta_C)^{-1}(1+\rho_{I_{dist}}\theta_{I_{dist}}) \quad (23)$$

$$d_2(x,u,t) = -\omega i_1^q + \frac{\rho_L\theta_L}{\bar{L}}(Rx_2 - u + V_1^d)(1+\rho_L\theta_L)^{-1} \quad (24)$$

$d1(x,t)$ is named as matched uncertainty whereas $d2(x,u,t)$ is unmatched uncertainty, according to nonlinear control terminology [30]. Thus, the system is written in the following general standard form:

$$\dot{x}_n = a(x,t) + b(x,t)u(t) + d_n(x,u,t)$$

where, b=1$\bar{L}$. The disturbance in (25) is continuous
Step 2. Define the multiple surface sliding surfaces, as follows [30]:

$$s_j^* = s_j - s_j(0)e^{-\beta_j t}$$

$$s_j = x_j - x_{jd}$$

where, β is a positive constant value and xjd is the desired state trajectories. The purpose is to enforce each sliding surface $sj*$ to zero such that $xj \cong xjd$. Therefore, obtaining the derivative of the first sliding surfaces we have:

$$\dot{s}_1^* = \dot{s}_1 + s_1(0)\beta_1 e^{-\beta_1 t} = s_2 + x_{2d} + d_{l1} - \dot{x}_{1d}$$

The estimation error is defined as follows:

$$e_{d_{lj}} = d_{lj} - \tilde{d}_{lj}$$

Step 3. Design actual control law: Until now, the virtual control inputs were designed; they are $x1d$,$2d$. To stabilize the uncertain system (25), the following actual control input is proposed here as follows:

$$u = -\frac{1}{b(x,t)}\left(a(x,t) + \tilde{d}_{ln} - x_{1d}^{(n)} + \zeta_{ln}s_n^* + \zeta_s sat(s_n^*)\right)$$

Therefore;

$$u = -\bar{L}\left(a(x,t) + \tilde{d}_{l2} - \ddot{x}_{1d} + \zeta_{l2}s_2^* + \zeta_s sat(s_2^*)\right)$$

where, $\zeta l2$ is a linear gain, ζs is the switching gain and the hyperbolic tangent function is approximately equal to:

$$sat(s_2^*) = \begin{cases} sgn(s_2^*) & , \ if\ |s_2^*| > \varrho \\ \frac{s_2^*}{\varrho} & , \ if\ |s_2^*| \le \varrho \end{cases}$$

where, ϱ is a small positive constant. Substituting (32) in (29), the dynamics of the sliding surface $s2*$ is:

$$\dot{s}_2^* = -\zeta_{l2}s_2^* - \zeta_s sat(s_2^*)$$

Note that during obtaining the derivatives of the disturbances in the design procedure, the discrete control part had been excluded and did not appear in the derived equations. This is because when designing the SMC-based controller, the designed control signal contains two parts; the equivalent control energy $ueq$and a discrete part ud which is added to the obtained control signal to

make it robust against disturbances. Notice that during designing the controller and considering the disturbances, the design objective is to obtain the equivalent control energy law ueqbased on the Lyapunov energy function. Then, the discrete term ud is manually added to the control law to make the obtained signal robust. Therefore, the time derivative of the control law exists during the design process. For more details please refer to [33].

Step 4. Obtaining the disturbance observer dynamics: The NDO aims to estimates the disturbance $\tilde{d}li$ as follows:

$$\begin{cases} \tilde{d}_{lj} = p_j + \lambda_j s_j^* \\ \dot{p}_j = -\lambda_j \left(s_{(j+1)} + x_{(j+1)d} + \tilde{d}_{lj} - x_{1d}^{(j)} \right) \end{cases} \quad -(35)$$

where, pj and λj are a dummy variable and gains of the observer, respectively. Calculating the derivative of $\tilde{d}\ lj$ we get:

$$\tilde{d}_{lj}^{(1)} = \dot{p}_j + \lambda_j \dot{s}_j^* = -\lambda_j \left(s_{(j+1)} + x_{(j+1)d} + \tilde{d}_{lj} - x_{1d}^{(j)} \right) +$$
$$\lambda_j \left(s_{(j+1)} + x_{(j+1)d} + d_{lj} - x_{1d}^{(j)} \right) = \lambda_j (d_{lj} - \tilde{d}_{lj}) = \lambda_j e_{d_{lj}} \quad (36)$$

and;

$$\|\dot{d}_l\| \leq \gamma \quad (37)$$

Step 5. Stability proof: The Lyapunov function is defined as:

$$V_1(e_{d_l}) = {e_{d_l}}^T P e_{d_l}$$

Calculating the derivative of Lyapunov function and using Equations (34)-(36) we get:

$$\dot{V}_1 = {e_{d_l}}^T (D^T P + PD) e_{d_l} + 2 {e_{d_l}}^T P \dot{d}_l \leq -{e_{d_l}}^T Q e_{d_l} +$$
$$2\|e_{d_l}\| . \|P\| . \|\dot{d}_l\|$$

where, $D = diag[\lambda \quad \lambda]$ Q is a positive arbitrary matrix, and P is a positive matrix such that the following constraint is satisfied.

$$D^T P + PD = -Q \quad (40)$$

Analytically:

$$P = \begin{bmatrix} P_{11} & P_{12} \\ P_{12}^T & P_{22} \end{bmatrix} \quad (41)$$

and we have:

$$\begin{bmatrix} \lambda_1 & 0 \\ 0 & \lambda_2 \end{bmatrix} \begin{bmatrix} P_{11} & P_{12} \\ P_{12}^T & P_{22} \end{bmatrix} + \begin{bmatrix} P_{11} & P_{12} \\ P_{12}^T & P_{22} \end{bmatrix} \begin{bmatrix} \lambda_1 & 0 \\ 0 & \lambda_2 \end{bmatrix} = -Q \quad (42)$$

Therefore, considering Q as an identical matrix, and using (30) and (35)-(37), e_{d_l} will be bounded by;

$$\|e_{d_l}\| \leq \lambda_l \quad (43)$$

where;

$$\lambda_l = \frac{2\|P\|\gamma}{\lambda_m} \quad (44)$$

and the system is robustly stable.

4.Neural network:

A neural network is a network or circuit of neurons, or in a modern sense, an artificial neural network, composed of artificial neurons or nodes.[1] Thus a neural network is either a biological neural network, made up of real biological neurons, or an artificial neural network, for solving artificial intelligence (AI) problems. The connections of the biological neuron are modeled as weights. A positive weight reflects an excitatory connection, while negative values mean inhibitory connections. All inputs are modified by a weight and summed. This activity is referred to as a linear combination. Finally, an activation function controls the amplitude of the output. For example, an acceptable range of output is usually between 0 and 1, or it could be −1 and 1.

These artificial networks may be used for predictive modeling, adaptive control and applications where they can be trained via a dataset. Self-learning resulting from experience can occur within networks, which can derive conclusions from a complex and seemingly unrelated set of information.

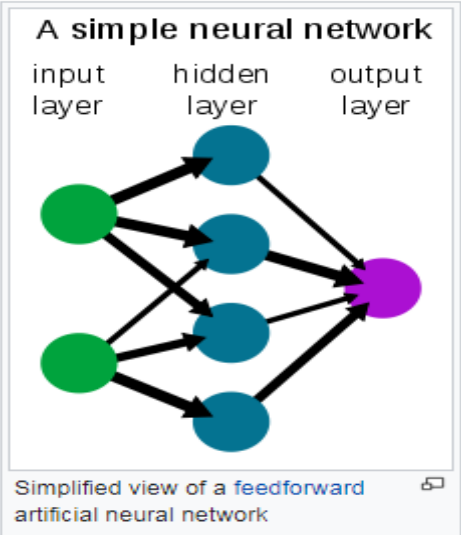

Simplified view of a feedforward artificial neural network

Artificial intelligence:

A neural system (NN), on account of counterfeit neurons called fake neural system (ANN) or mimicked neural system (SNN), is an interconnected gathering of regular or fake neurons that utilizes a scientific or computational model for data preparing dependent on a connectionistic way to deal with calculation. Much of the time an ANN is a versatile framework that changes its

structure dependent on outer or inward data that moves through the system. In more reasonable terms neural systems are non-straight factual information displaying or dynamic instruments. They can be utilized to display complex connections among information sources and yields or to discover designs in information. A counterfeit neural system includes a system of basic preparing components (fake neurons) which can show complex worldwide conduct, controlled by the associations between the handling components and component boundaries. Fake neurons were first proposed in 1943 by Warren McCulloch, a neurophysiologist, and Walter Pitts, a rationalist, who originally teamed up at the University of Chicago.

One old style kind of counterfeit neural system is the repetitive Hopfield organize.

The idea of a neural system seems to have first been proposed by Alan Turing in quite a while 1948 paper Intelligent Machinery in which called them "B-type chaotic machines".

The utility of fake neural system models lies in the way that they can be utilized to gather a capacity from perceptions and furthermore to utilize it. Unaided neural systems can likewise be utilized to learn portrayals of the information that catch the remarkable qualities of the information appropriation, e.g., see the Boltzmann machine (1983), and all the more as of late, profound learning calculations, which can verifiably gain proficiency with the dissemination capacity of the watched information. Learning in neural systems is especially helpful in applications where the unpredictability of the information or errand makes the plan of such capacities by hand unfeasible..

Applications: Neural systems can be utilized in various fields. The errands to which counterfeit neural systems are applied will in general fall inside the accompanying general classes:

Function estimate, or relapse examination, including time arrangement expectation and displaying.

- Classification, including example and grouping acknowledgment, oddity recognition and successive dynamic.
- Data handling, including sifting, grouping, dazzle signal partition and pressure.

Application territories of ANNs incorporate nonlinear framework identification[19] and control (vehicle control, process control), game-playing and dynamic (backgammon, chess, dashing), design acknowledgment (radar frameworks, face ID, object acknowledgment), grouping acknowledgment (motion, discourse, transcribed content acknowledgment), clinical conclusion, monetary applications, information mining (or information revelation in databases, "KDD"), perception and email spam sifting. For instance, it is conceivable to make a semantic profile of client's inclinations rising up out of pictures prepared for object acknowledgment.

Neuroscience:

Hypothetical and computational neuroscience is the field worried about the hypothetical examination and computational displaying of natural neural frameworks. Since neural frameworks are personally identified with intellectual procedures and conduct, the field is firmly identified with psychological and social displaying.

The point of the field is to make models of natural neural frameworks so as to see how organic frameworks work. To pick up this understanding, neuroscientists endeavor to make a connection between watched natural procedures (information), organically conceivable instruments for neural handling and learning (organic neural system models) and hypothesis (factual learning hypothesis and data hypothesis).

Types of models

Numerous models are utilized; characterized at various degrees of deliberation, and displaying various parts of neural frameworks. They go from models of the transient conduct of individual neurons, through models of the elements of neural hardware emerging from cooperations between singular neurons, to models of conduct emerging from conceptual neural modules that speak to finish subsystems. These incorporate models of the long haul and transient pliancy of neural frameworks and its connection to learning and memory, from the individual neuron to the framework level..

SIMULATION RESULTS:

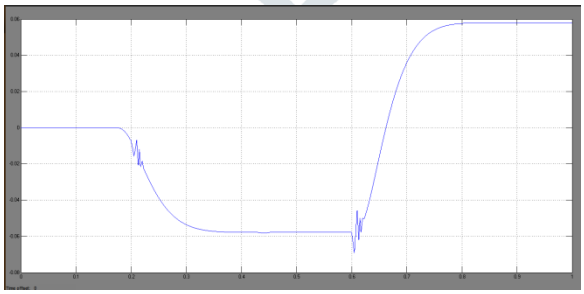

VSE Series Injected Voltage

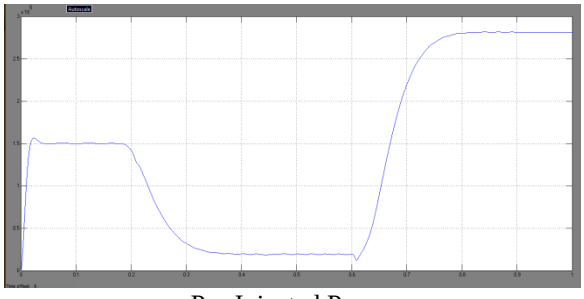

Pse Injected Power

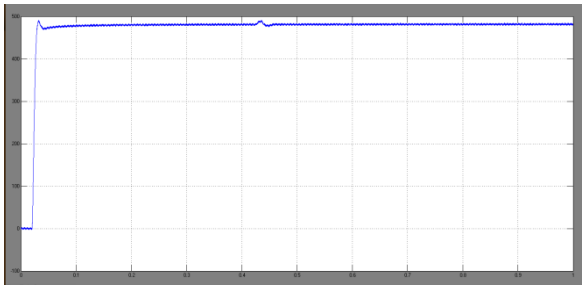

Dc LINK VOLTAGE

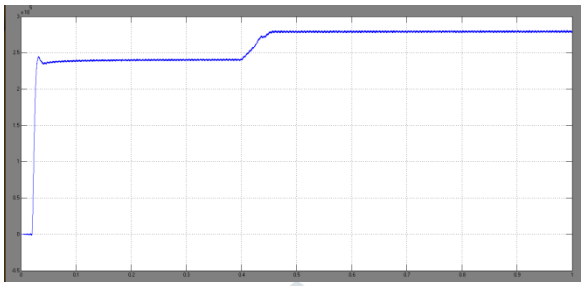

Fig. 14. Active power of DC link when 40 kW is demanded from the AC side

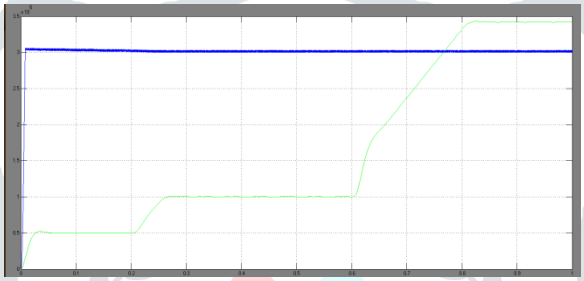

Fig. 13. Generation in each micro grid

Simulation results with Neural Nework Controller:

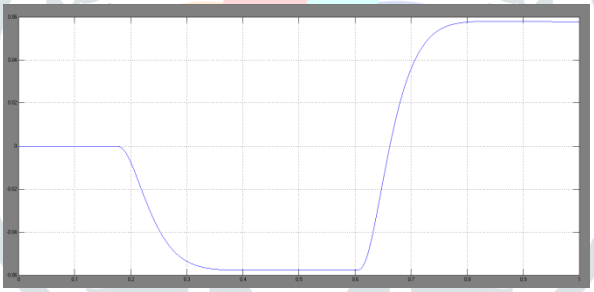

VSE Series Injected Voltage

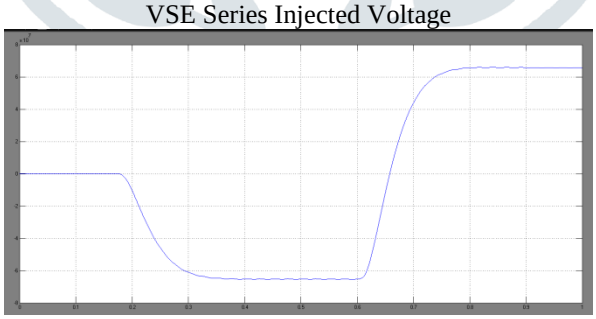

Pse Injected Power

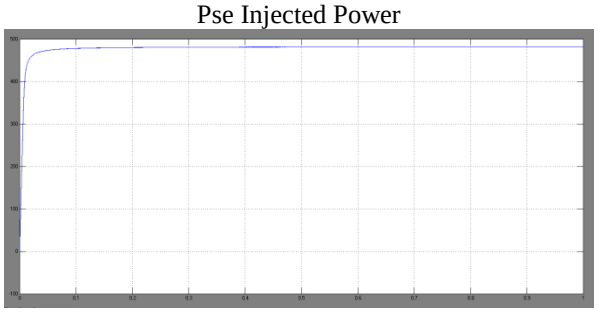

Dc LINK VOLTAGE

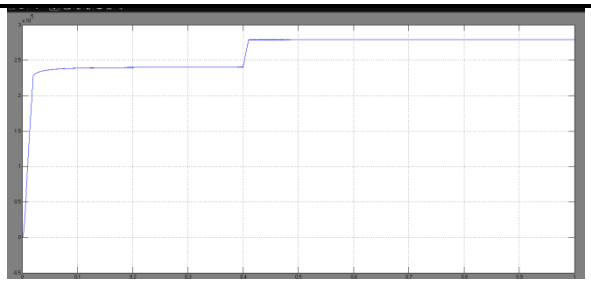

Fig. 14. Active power of DC link when 40 kW is demanded from the AC side

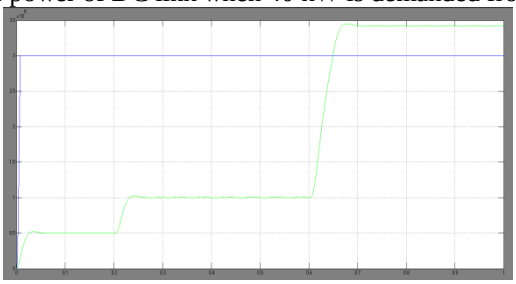

Fig. 13. Generation in each micro grid

V.CONCLUSION:

The hybrid microgrid structure is the most probable option in the future smart grids to gather together the renewable resources as well as AC/DC loads. This is due to the fact that this structure has the merits of both AC and DC microgrids simultaneously. One conventional problem with this structure is the power exchange control between interconnected AC and DC microgrids. In this study, a UIPC based solution has been proposed as a superior alternative to the parallel-connected power converters which have brought many problems. A modified structure of the UIPC has firstly been proposed and then effective control strategies have been introduced for the modified UIPC. The simulation results validated the modified model as well as the power exchange control performance between AC and DC microgrids. The performance of the system with Neural Network controller is better than the fuzzy logic controller.

VI. REFERENCES

[1] Runfan Zhang, Branislav Hredzak, "Distributed Finite-Time Multi-Agent Control for DC Microgrids with Time Delays", IEEE Transactions on Smart Grid, Early Access, 2018.

[2] Kumar Utkarsh, et al, "Distributed Model-predictive Real-time Optimal Operation of a Network of Smart Microgrids", IEEE Transactions on Smart Grid, Early Access, 2018.

[3] Haifeng Qiu, et al, " Bi-level Two-stage Robust Optimal Scheduling for AC/DC Hybrid Multi-microgrids", IEEE Transactions on Smart Grid, Early Access, 2018.

[4] Pengfeng Lin, et al, "A Distributed Control Architecture for Global System Economic Operation in Autonomous Hybrid AC/DC Microgrids", IEEE Transactions on Smart Grid, Early Access, 2018.

[5] Daniel E. Olivares, et al, "Trends in Microgrid Control", IEEE Transactions on Smart Grid Volume: 5, Issue: 4, pp. 1905 – 1919, 2014.

[6] Jongwoo Choi, et al, "Robust Control of a Microgrid Energy Storage System using Various Approaches", IEEE Transactions on Smart Grid, Early Access, 2018.

Authors profile:

K Umamaheswar Reddy currently persuing post graduation at quba college of engineering and technology, venkatachalam, nellore. A,P.

M.Ramu received graduate degree in Electrical And Electronics Engineering in sri skr college of engineering and technology manubolu, spsr nellore district and post graduation degree specialisation of electrical power systems in N.B.K.R institute of science and technology vidyanagar, nellore and presently working as assistant professor in EEE department at QUBA college of engineering and technology venkatachalam, nellore A.P